SOLAR ASSISTED RELIFT LUO CONVERTER WITH UPQC FOR VOLTAGE UNBALANCE MITIGATION USING DDSRF THEORY

B Pakkiraiah, Associate Professor, SMIEEE, Dept. of EEE, Gokaraju Rangaraju Institute of Engineering and Technology-Autonomous, Hyderabad-500090, India, Email: *pakki1988@gmail.com*

M.Venkateswarlu, Research Scholar, Department of EEE, Koneru Lakshmaiah Education Foundation, Vaddeswaram, Guntur, Andhra Pradesh 522502, India, Email: *malapativenkateswarlu9@gmail.com*

B Loveswara Rao, Professor, Dept. of EEE, Koneru Lakshmaiah Education Foundation, Vaddeswaram, Guntur, Andhra Pradesh 522502, India, Email: *allenblovesh@gmail.com*

Abstract-The upsurge seen in integration of sensitive non-linear loads and Photovoltaic (PV) system based power generation has strengthened the demand for enhanced Power Quality (PQ) in distributed power system. Thereby, a Unified Power Quality Conditioner (UPQC), which is a custom power device is proposed in this work for improving the PQ of the overall network. The load side PQ issues is mitigated using the shunt compensator, while the source side PQ issues is mitigated using the series compensator of the UPQC. The active power to the load is provided from the PV system through a shunt compensator. The voltage level of the output obtained from the PV is improved with the aid of Re-lift Luo converter, which is a DC-DC converter of high efficiency and voltage gain. Moreover, in order to provide a stabilized voltage supply to the UPQC, an Adaptive Proportional Integral (PI) controller is selected and its gains are adjusted with the application of Fuzzy Logic Controller (FLC). The Decoupled Double Synchronous Reference Frame (DDSRF) theory is applied to derive the reference voltage and reference current for balancing source voltage variations and load current harmonics, respectively. The series and shunt compensators are controlled using Cascaded Type-2 FLC (CT2FLC). The effectiveness of the proposed PV-UPQC configuration in eliminating load current harmonics and source voltage fluctuations is evaluated on the basis of MATLAB simulations.

Keywords: PV-UPQC, Re-lift Luo converter, DDSRF Theory, Adaptive PI controller, CT2FLC

I   INTRODUCTION

The Power Quality (PQ) is instrumental in guaranteeing the proper working of several electronic and electrical devices used in industrial, commercial and domestic applications. Moreover, poor PQ augments the energy costs and negatively impacts the operation of the advanced sensitive equipment coupled to the network. Consequently, in order to avert the failure of these devices, the electrical grid must provide power within the ranges established by manufacturers [1, 2]. The property of drawing non-linear current by the power electronic loads is the major cause of PQ issues in the form of voltage fluctuations in the distribution system [3]. Furthermore, the focus on producing clean energy has increased the prevalence of PV in distributed power systems, which in turn causes voltage instability issues because of its intermittent nature. These voltage instability issues effectuates persistent false triggering, false tripping and malfunctioning of the electronic systems in addition to capacitor bank heating [4, 5]. Thereby, the development of a multifunctional system, which satisfies the requirement of both clean energy generation and PQ enhancement is the major objective of this work. In [6], a multifunctional three phase solar energy conversion system is proposed, which has the capability to compensate the PQ issues in load side. A Distribution Static Compensator (DSTATCOM) based shunt active filtering in addition to clean energy generation is proposed in [7], [8]. The benefit of excellent load voltage regulation by DSTATCOM comes at the cost of reactive power injection. As a result, DSTATCOM is unable to simultaneously maintain grid current unity power factor and PCC voltage

1906

regulation. Recently, the use of Dynamic Voltage Resonator (DVR) [9], which is a series active filtering device is recommended to adhere to the strict PQ requirements of sensitive electronic loads.

For obtaining the additional advantage of decarbonized energy generation, PV based DVR configurations are developed in [10], [11]. In comparison to DVR and DSTATCOM, an UPQC [12, 13], which performs both shunt active filtering and series active filtering is preferred. Utilization of a suitable controller approach in cooperation with a DC-DC converter allows for the elimination of the intermittency-related limitation of the PV system. The former stabilizes the high voltage output of the latter by regulating its duty cycle. A Re-lift Luo converter is selected for improving the voltage level of the PV system. The widely used linear controller approach for controlling the working of a power electronic converter is PI controller. However, the nature of being a fixed gain controller, limits its adaption capability to deviations in environmental factors and system parameters.

Therefor an FLC is employed for tuning the gain values of the PI controller for enhancing its dynamic response and expanding its application in wide span of operating conditions [14-16]. The technique of cascaded control [17] entailing two T2FLC [18, 19] is proposed for controlling the UPQC. The major task of reference signal generation is accomplished using DDSRF Theory.   In this work, a PV-UPQC that supports enhanced PQ as well as carbon negative power generation is presented. A stabilized, controlled and enhanced voltage level is obtained from PV system with the application of Re-lift Luo converter and Fuzzy tuned Adaptive PI controller. A CT2FLC in addition to DDSRF theory is used for establishing control over the working of series and shunt compensators of the UPQC.

II   PROPOSED SYSTEM DESCRIPTION

The foremost responsibility of a utility system is to provide electric power in the form of pure sinusoidal current and voltage of suitable frequency and magnitude at PCC to the customers. So, a PV-UPQC for enhancing the PQ of the distributed power system is presented with the added benefit of carbon free power generation.
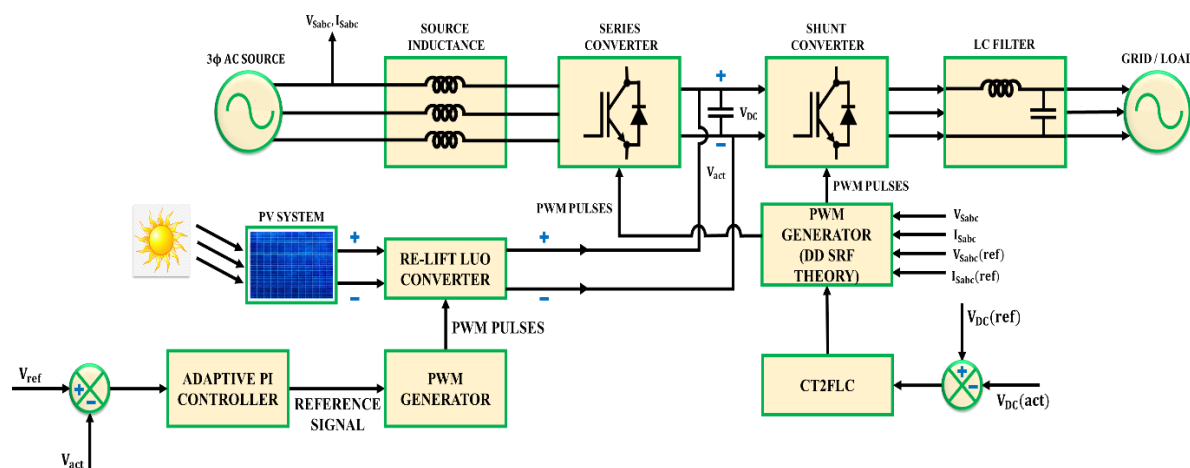

Figure 1: Presented configuration of PV-UPQC

The PV is interfaced to the UPQC using the Re-lift Luo converter and its output is stabilized with the aid of fuzzy tuned Adaptive PI controller. The value of error obtained after comparing the set reference voltage with the actual voltage of the Re-lift Luo converter is provided as input to the

1907

Adaptive PI controller. The reference control signal generated by the controller aids the PWM generator to produce pulses for governing the switches of the Re-lift Luo converter. In case of UPQC, the series converter mitigates the voltage quality issues in the source side, while the shunt converter mitigates the current harmonics issues in load side. The reference and actual DC-link voltage ($V_{DC}(ref), V_{DC}(act)$) are compared and the evaluated error in voltage is fed to the CT2FLC for processing. The reference voltage signal for stabilizing source voltage fluctuations and the reference current signal for minimizing the load side current harmonics is generated based on DDSRF theory. Finally using the proposed configuration of PV-UPQC the PQ of both source side and load side is enhanced.

III   PROPOSED SYSTEM MODELLING

A) PV FED RE-LIFT LUO CONVERTER

The PV module that encompasses numerous PV cells is designed on the basis of single diode model as seen in Figure 2. Moreover, the output current derived from the PV cell is given as,

$$I_{pv} = I_{ph} - I_0 \left[exp\left(\frac{q(V+IR_s)}{N_s KTA} \right) - 1 \right] - (V + IR_s)/(R_p) \tag{1}$$

Here, I_0 specifies the reverse saturation current of the diode, A specifies the diode Ideality constant, q specifies the electron charge, K specifies the Boltzmann constant, I_{pv} and I_{ph} specifies the PV generated current and the photo generated current respectively and moreover, the terms R_p and R_s represents the shunt and series resistances respectively.
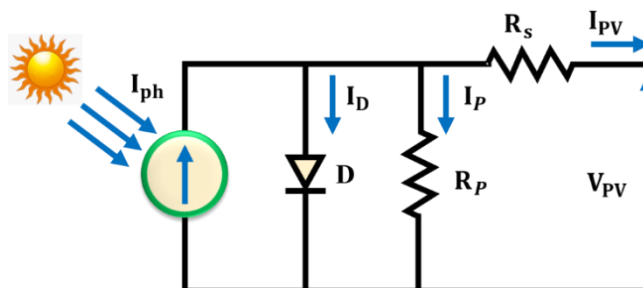

Figure 2: PV cell

Re-Lift Luo converter as seen in Figure 3 comprises of three diodes D_a, D_b, D_c; three capacitors C_a, C_b, C_c; three inductors L_a, L_b, L_c; two power switches S_1, S_2 and an output capacitor C_o as shown in Figure 2. Capacitors C_b and C_c possess voltage boosting characteristics which makes the capacitor voltage V_C higher than the source voltage V_{PV}. The inductor L_c serves as a ladder joint for connecting the capacitors C_b and C_c in order to raise the capacitor voltage V_{C_a}. The operating modes and operational waveform of the Re-Lift Luo converter is given in Figure 4 and Figure 5 respectively.
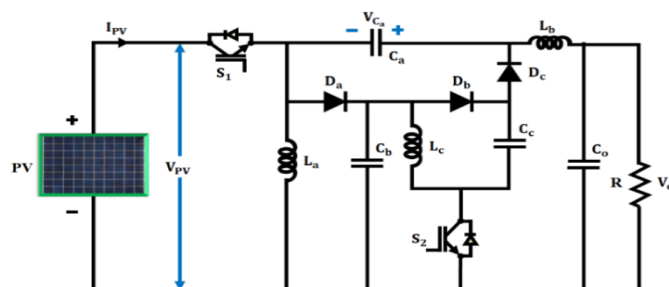
1908

Eur. Chem. Bull. 2023,12(5), 1906-1924

Figure 3: Configuration of Re-lift Luo converter

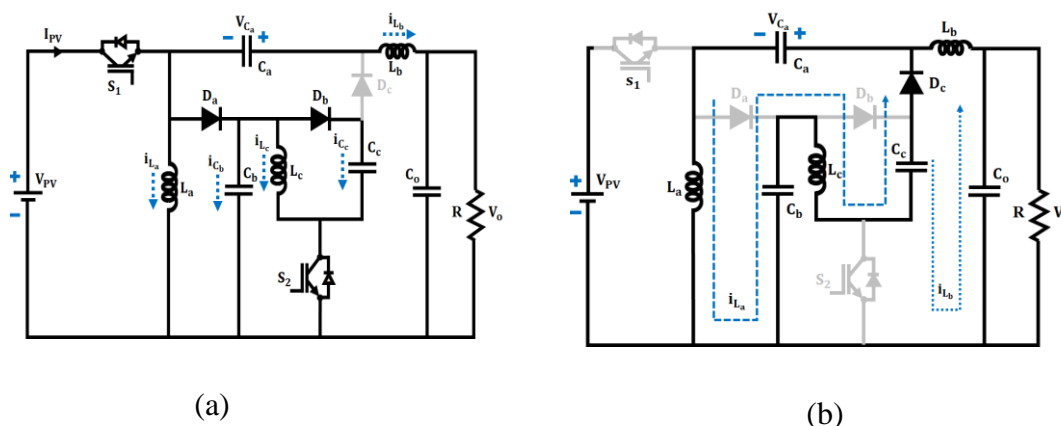(a)   (b)

Figure 4: Re-lift Luo converter operating modes

Mode 1:

Throughout this mode, both the switches are in ON condition and the source energy is absorbed by the inductors L_a and L_c. The energy for the inductor L_b is obtained from both the input source and capacitor C_a. A linear increase in currents i_{L_a}, i_{L_b} and i_{L_c} is seen in this mode.

Mode 2:

Unlike mode 1, both the switches are in OFF condition and the source current I_{PV} is equivalent to zero. The capacitor C_a is charged by the current i_{L_a}, which means that the stored energy from inductor is transferred to the capacitor C_a. Both the currents i_{L_a} and i_{L_b} decreases throughout this mode.

During mode 1, the peak to peak variation of current i_{L_c} is given as,

$$\Delta i_{L_c} = \frac{V_{PV}kT}{L_c}$$

(2)

The variation is equivalent to the current reduction during mode 2,

$$\Delta i_{L_c} = \frac{V_{L_c}(1-k)T}{L_c}$$

(3)

The drop in voltage across inductor L_c is during mode 2 is given as,

$$V_{L_c} = \frac{k}{1-k}V_{PV}$$

(4)

1909

The current i_{L_a} increases during the time period kt [mode 1] and a decreases during the time period $(1-k)t$ [mode 2]

$$kTV_{PV} = (1-k)T(V_{C_a} - 2V_{PV} - V_{L_c})$$ (5)

The voltage across capacitor V_{C_a} is give as,

$$V_{C_a} = \frac{2}{1-k}V_{PV}$$ (6)

Moreover, the current i_{L_h} also increases throughout mode 1 and decreases in mode 2. Hence,

$$kT(V_{C_a} + V_{PV} - V_o) = (1-k)T(V_o - 2V_{PV} - V_{L_c})$$ (7)

The output voltage V_o is given as,

$$V_o = \frac{2}{1-k}V_{PV}$$ (8)

The output current is given as,

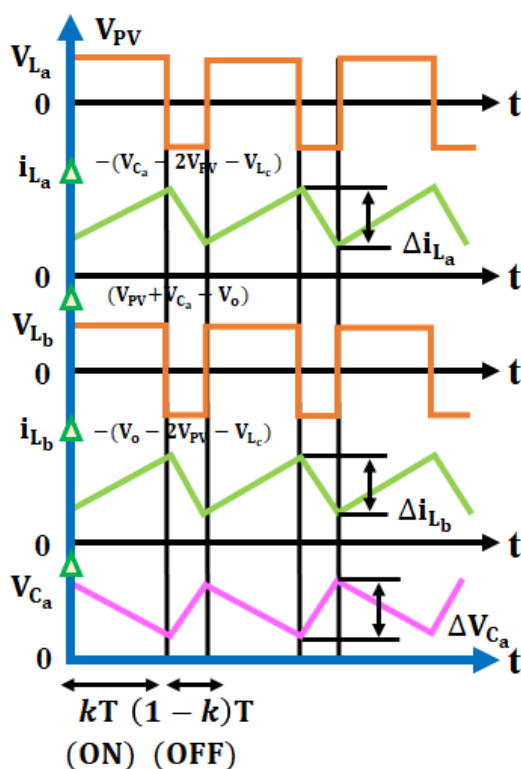$$I_o = \frac{1-k}{2}I_{PV}$$ (9)

Figure 5: Operational waveform of Re-Lift Luo converter

The value of the inductor L_a is,

1910

$$L_a = \frac{kTV_{PV}}{\Delta i_{L_a}}$$

(10)

The value of the inductor L_b is,

$$L_b = \frac{kTV_{PV}}{\Delta i_{L_b}}$$

(11)

The following equations are used to calculate the values of the capacitors C_a, C_b, C_c and C_o:

$$C_a = \frac{(1-k)Ti_{L_a}}{\Delta V_{C_a}} = \frac{(1-k)kT}{\Delta V_{C_a}}I_{PV}$$

(12)

$$C_b = \frac{(1-k)T(i_{L_a}+i_{L_b})}{\Delta V_{C_h}} = \frac{I_o T}{\Delta V_{C_h}}$$

(13)

$$C_c = \frac{(1-k)T(i_{L_a}+i_{L_b})}{\Delta V_{C_c}} = \frac{I_o T}{\Delta V_{C_c}}$$

(14)

$$C_o = \frac{kT^2 V_{PV}}{4\Delta V_o L_b}$$

(15)

In order to enhance the transient response of the Re-lift Luo converter, a fuzzy tuned PI controller is adopted in this research.

B) FUZZY TUNED ADAPTIVE PI CONTROLLER

The preferable characteristics of conventional PI controller such as quick response and ease of implementation accredits to its widespread usage in variety of industrial applications. The property of being a fixed gain controller, however, hampers its adaption capability to deviations in environmental factors and system parameters. Consequently, an Adaptable PI controller, which incorporates the independent and adaptive qualities of FLC with the aspect of rapid response of a PI controller, is employed in this work. In contrast to conventional PI controller, the gains K_P and K_I are adjustable rather than being fixed and these gains are estimated by using the FLC. Figure 6 gives the configuration of the Re-lift Luo converter with Adaptive PI controller.
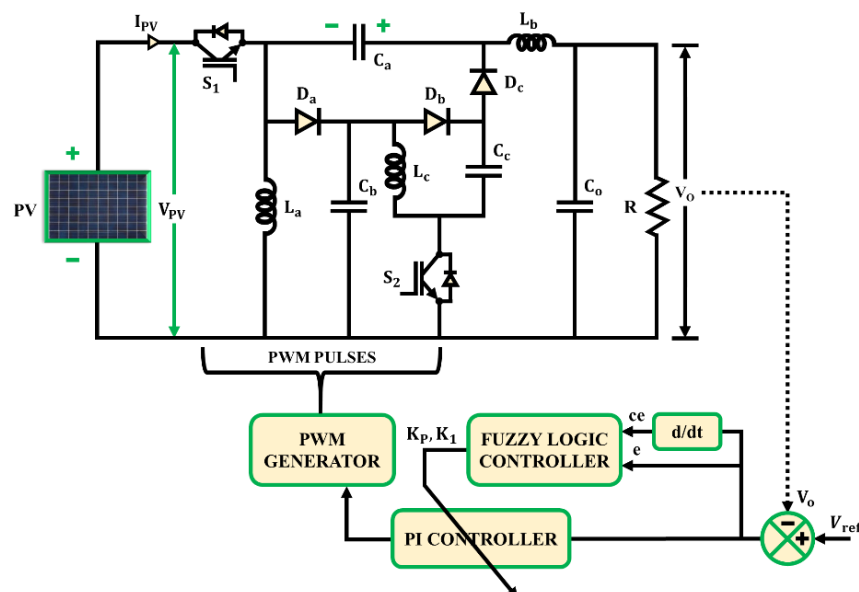
1911

Eur. Chem. Bull. 2023,12(5), 1906-1924

Figure 6: Adaptive PI controller for Re-lift Luo converter

Table 1: Rule base for PI gains

Output	Error (e)				
(K_P)		NL	NS	Z	PS	PL
Change in Error (ce)	NL	L	L	M	M	S
	NS	L	L	M	S	S
	Z	M	M	M	M	M
	PS	S	M	M	M	L
	PL	S	S	M	L	L
Output	Error (e)				
(K_I)		NL	NS	Z	PS	PL
Change in Error (ce)	NL	S	S	M	L	L
	NS	S	S	M	L	L
	Z	M	M	M	M	M
	PS	L	L	M	S	S
	PL	L	L	M	S	S

The adaptive PI controller is selected with the aim of controlling the output voltage of the Re-lift Luo converter, therefore the input variables for the FLC are given as the voltage error (e) and change in voltage error (ce). Each of these two input variables are assigned with five triangular membership functions as illustrated in Figure 7 (a). The fuzzy variables for the inputs are expressed using the linguistic variables Negative Large (NL), Negative Small (NS), Zero (Z), Positive Small (PS) and Positive Large (PL). The process of fuzzy inference and defuzzification is accomplished using Min-Max technique and centre of gravity respectively. The FLC has two rule bases as seen in Table 1 for estimating the values of the PI gains $K_P \; and \; K_I$. The membership functions used for estimating the

1912

output variables K_P and K_I are expressed using the linguistic variables Large (L), Medium (M) and Small (S) as seen in Figure 7(b).
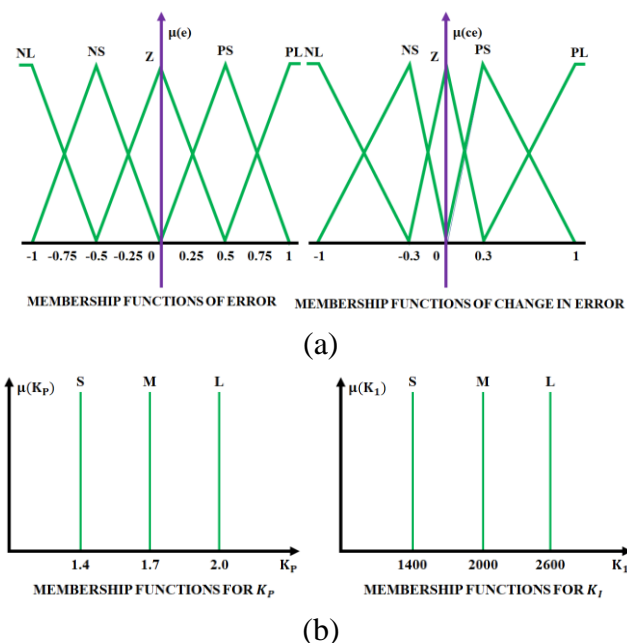

(a)

(b)

Figure 7: Membership functions of (a) Input Variables and (b) Output Variables

The rules are developed based on knowledge of functioning of the converter, error variations and change in error inputs. For each rule i, the firing strength is given as,

$$\mu_i = \prod_{j=1}^{2} A_{ij} \tag{16}$$

Where, A_{ij} refers to the membership function. The singleton values are represented using the terms c_i and v_i. The outs obtained from the FLC is given as,

$$K_P = \frac{\sum_{i=1}^{r} c_i \mu_i}{\sum_{i=1}^{r} \mu_i} \tag{17}$$

$$K_I = \frac{\sum_{i=1}^{r} v_i \mu_i}{\sum_{i=1}^{r} \mu_i} \tag{18}$$

Where, the number of rules is given as r. Thus output signal obtained from the PI controller is given as,

$$u = K_P e + K_I \int e \, dt \tag{19}$$

Thus a stable output voltage is obtained from the Re-lift Luo converter, under all operating conditions with the assistance of FLC tuned adaptive PI controller.

C) MODELLING OF UPQC

The UPQC ensures that a power of appropriate standard and specification is supplied constantly without deviation to the loads coupled to the distributed power system. The load side PQ issues

1913

including reactive power and harmonics are scaled down with the aid of shunt compensator, whereas the grid side PQ issues such as sag/swell are scaled down with the aid of series compensator. Moreover, the former enhances the load side PQ with the injection of current and the latter enhances the grid side PQ through the injection of voltage. The parameters considered for designing the UPQC are,

DC-link Voltage Magnitude

On the basis of the system's phase voltage, the minimal value of the DC-link voltage is determined and is expressed as,

$$V_{dc,min} = \frac{2\sqrt{2}(V_{LL,rms})}{\sqrt{3}(m)} \tag{20}$$

Where, the grid's phase-voltage is specified as $V_{LL,rms}$ and the modulation depth is specified as m.

Shunt Compensator DC-link Capacitor Value

The capacitance value of the DC-link capacitor is expressed using the following equation,

$$C_{dc,min} = \frac{3V_{ph}i_{sh}a_f k_e t}{1/2(V_{dc,ref}^2 - V_{dc,min}^2)} \tag{21}$$

Where, the shunt compensator's phase-current and phase-voltage is specified using the terms i_{sh} and V_{ph} respectively. The energy variation under dynamic condition is specified as k_e, overloading factor is specified as a_f and the reference voltage is specified as $V_{dc,ref}$.

Inductor Ripple Filter

The shunt compensator is interfaced to the network through an inductor, which is mathematically expressed as,

$$L_{f,min} = \frac{(\sqrt{3})(m)(V_{dc,ref})}{12(a_f)(f_S)(I_{cr})} \tag{22}$$

Where, inductor ripple current is specified as I_{cr} and the switching frequency is specified as f_S.

Series Injection Transformer

In case of a series transformer, the injection transformer's maximum value turns ratio is given as,

$$K_{SE} = \frac{V_{LLrms}}{\sqrt{3}(V_{SE})} \tag{23}$$

The transformer's VA rating is given as,

$$S_{SE} = 3(V_{SE})(i_{SE_{(under\ sag)}}) \tag{24}$$

The grid current is equivalent to current across series compensator.

Series Compensator Inductor Ripple Filter

1914

Eur. Chem. Bull. 2023,12(5), 1906-1924

The inductor ripple filter is given as,

$$L_{r,min} = \frac{(\sqrt{3})(m)(V_{dc,ref})(K_{SE})}{12(a_f)(f_S)(I_r)}$$

$$(25)$$

Where, inductor ripple current is specified as I_r. The control of both the series and shunt compensator is enabled using DDSRF theory and CT2FLC.

D) MODELLING OF CT2FLC

The control of the operation of UPQC is entrusted with CT2FLC, which comprises of two Type 2-FLC (T2FLC). In contrast to its counterpart, the T1-FLC, the T2-FLC is used in this work because it is better suited to handle challenges involving non-linearity and uncertainty. The control signal originating from the first T2FLC is used as input for the second T2FLC.
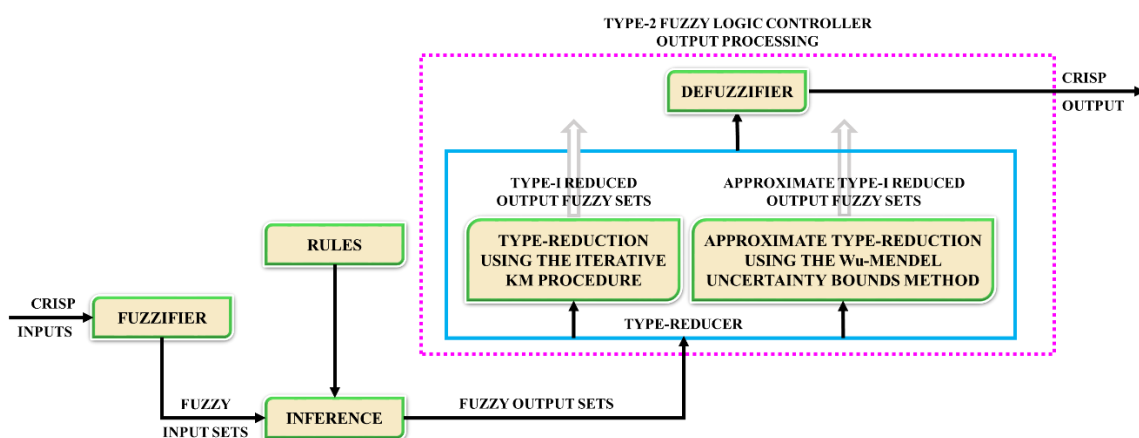

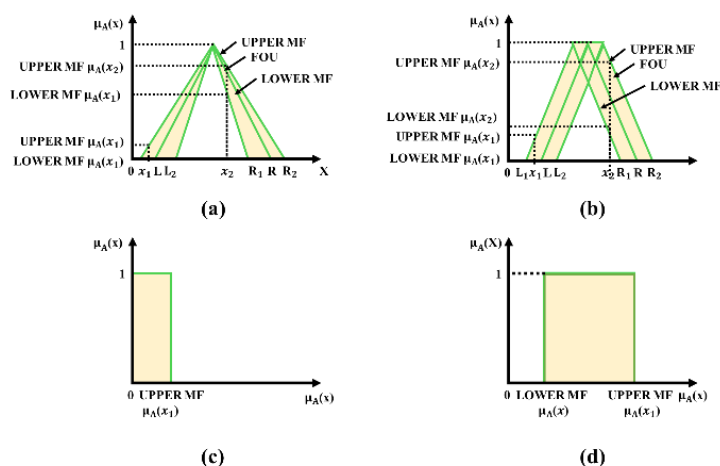**Figure 8:** Configuration of T2FLC

Figure 9: T2FLC FOU (a)

Figure 8 gives the configuration of T2FLC, which is a natural extension of T1FLC but gives additional information in the secondary membership function. Additionally, the former varies from the later in terms of structure by having an output processing block in place of the defuzzifier block. The defuzzification block is present within the output processing module along with a type reducer. As seen

1915

in Figure 9, it uses the concept of footprint of uncertainty (FOU). The role of the fuzzification block is to generate T2 fuzzy sets $\widetilde{A}_x$ by converting the input numeric vector $X = (x_1, x_2, ..., x_p)^T \in X_1 \times X_2 \times ... \times X_p \equiv X$. The mapping of the input is given as,

$$\mu_{\widetilde{A}_x}(x) = 1/1 \ and \ x = x' \tag{26}$$

$$\mu_{\widetilde{A}_x}(x) = 1/0 \ for \ \forall x \in x \ with \ x \neq x' \tag{27}$$

The rule structure of T2FLC is expressed as,

$$R^i: IF x_1 is \widetilde{F^i_1} and ... and \ x_p \ is \ \widetilde{F^i_p}, THEN \ Y^i = C^i_0 + C^i_1 x_1 + ... + C^i_p x_p \tag{28}$$

Where, $C^i_j(j = 0,1, ..., p)$ and $\widetilde{F^i_k}(k = 1, ..., p)$ represents T1 consequent and T2 antecedent fuzzy sets respectively. The output is specified as Y^i. The fuzzy sets are used for producing mappings by the inference engine. These mappings are realized by computing union and intersection operations. On the basis of the type reduced set (Y_1, Y_r) obtained from the type reducer, the evaluation of the output of the defuzzifier is carried out, which is given as,

$$y(x) = \frac{y_1 + y_r}{2} \tag{29}$$

Thus the CT2FLC is used for controlling the working of the UPQC.

E) DDSRF THEORY

The equation that represents the negative, positive and zero component of a three phase power system is given as,

$$\begin{bmatrix} V_{as} \\ V_{bs} \\ V_{cs} \end{bmatrix} = V_0 \begin{bmatrix} y(\omega t + \phi_0) \\ y(\omega t + \phi_0) \\ y(\omega t + \phi_0) \end{bmatrix}_+ V_1 \begin{bmatrix} y(\omega t + \phi_1) \\ y(\omega t - \frac{2\pi}{3} + \phi_1) \\ y(\omega t + \frac{2\pi}{3} + \phi_1) \end{bmatrix}_+ V_2 \begin{bmatrix} y(\omega t + \phi_2) \\ y(\omega t - \frac{2\pi}{3} + \phi_2) \\ y(\omega t + \frac{2\pi}{3} + \phi_2) \end{bmatrix} \tag{30}$$

The unsymmetrical source voltage is represented as,

$$V_s = \begin{bmatrix} V_{as} \\ V_{bs} \\ V_{cs} \end{bmatrix} = \begin{bmatrix} V_{a0} \\ V_{b0} \\ V_{c0} \end{bmatrix}_+ \begin{bmatrix} V_{a1} \\ V_{b1} \\ V_{c1} \end{bmatrix}_+ \begin{bmatrix} V_{a2} \\ V_{b2} \\ V_{c2} \end{bmatrix} \tag{31}$$

The source current component is given as,

$$I_s = \begin{bmatrix} I_{as} \\ I_{bs} \\ I_{cs} \end{bmatrix} = \begin{bmatrix} I_{a0} \\ I_{b0} \\ I_{c0} \end{bmatrix}_+ \begin{bmatrix} I_{a1} \\ I_{b1} \\ I_{c1} \end{bmatrix}_+ \begin{bmatrix} I_{a2} \\ I_{b2} \\ I_{c2} \end{bmatrix} \tag{32}$$

Using Clark's transformation, the three-phase voltage is transformed as,

1916

Eur. Chem. Bull. 2023,12(5), 1906-1924

$$V_{\alpha\beta 0} = \frac{2}{3}\begin{bmatrix} 1 & -\frac{1}{2} & -\frac{1}{2} \\ 0 & \frac{\sqrt{3}}{2} & -\frac{\sqrt{3}}{2} \\ \frac{1}{2} & \frac{1}{2} & \frac{1}{2} \end{bmatrix} V_s \tag{33}$$

Using Clark's transformation, the three-phase current is transformed as,

After eliminating the zero-sequence component,

$$V_{\alpha\beta} = \frac{2}{3}\begin{bmatrix} 1 & -\frac{1}{2} & -\frac{1}{2} \\ 0 & \frac{\sqrt{3}}{2} & -\frac{\sqrt{3}}{2} \end{bmatrix} V_s \tag{35}$$

$$1I_{\alpha\beta 0} = \frac{2}{3}\begin{bmatrix} 1 & -\frac{1}{2} & -\frac{1}{2} \\ 0 & \frac{\sqrt{3}}{2} & -\frac{\sqrt{3}}{2} \\ \frac{1}{2} & \frac{1}{2} & \frac{1}{2} \end{bmatrix} I_s \tag{34}$$

$$I_{\alpha\beta 0} = \frac{2}{3}\begin{bmatrix} 1 & -\frac{1}{2} & & & -\frac{2}{\quad} \\ 0 & \frac{\sqrt{3}}{2} & & & -\frac{\sqrt{3}}{2} \end{bmatrix} I_s \tag{36}$$

The real and imaginary power is given as,

$$\begin{bmatrix} p \\ q \end{bmatrix} = \begin{bmatrix} V_\alpha & V_\beta \\ -V_\beta & V_\alpha \end{bmatrix} \tag{37}$$

The resultant voltage is given as,

$$V_{\alpha\beta} = V_1\begin{bmatrix} \cos(\omega t + \phi_1) \\ \sin(\omega t + \phi_1) \end{bmatrix} + V_2\begin{bmatrix} \cos(-\omega t + \phi_2) \\ \sin(-\omega t + \phi_2) \end{bmatrix} \tag{38}$$

In stationary reference frame the voltage vector has the same frequency as the rotating coordinate system's angular frequency. By separating the positive and negative sequence components, a Park's transformation is used to determine the state of DDSRF.

$$V_{dq1} = V_{\alpha\beta}\begin{bmatrix} \cos(\omega t) & -\sin(\omega t) \\ -\sin(\omega t) & \cos(\omega t) \end{bmatrix} \tag{39}$$

$$V_{dq2} = V_{\alpha\beta}\begin{bmatrix} -\cos(\omega t) & -\sin(\omega t) \\ \sin(\omega t) & -\cos(\omega t) \end{bmatrix} \tag{40}$$

On the basis of equation (39) and (40), it is confirmed that

$$V_{dq1} = -V_{dq2} \tag{41}$$

$$V_{dq1} = V_1\begin{bmatrix} \cos(\phi_1) \\ \sin\phi_1 \end{bmatrix} + V_2\begin{bmatrix} \cos(\phi_2) & \sin(\phi_2) \\ -\sin(\phi_2) & \cos(\phi_2) \end{bmatrix}\begin{bmatrix} \cos(2\omega t) \\ \sin(2\omega t) \end{bmatrix} \tag{42}$$

1917

Eur. Chem. Bull. 2023,12(5), 1906-1924

$$V_{dq1} = V_1 \begin{bmatrix} \cos(\phi_1) \\ \sin\phi_1) \end{bmatrix} + V_{d2} \begin{bmatrix} \cos(2\omega t) \\ -\sin(2\omega t) \end{bmatrix} + V_{q2} \begin{bmatrix} \sin(2\omega t) \\ \cos(2\omega t) \end{bmatrix} \tag{43}$$

$$V_{dq2} = V_2 \begin{bmatrix} \cos(\phi_2) \\ \sin\phi_2) \end{bmatrix} - V_{d1} \begin{bmatrix} \cos(2\omega t) \\ \sin(2\omega t) \end{bmatrix} + V_{q1} \begin{bmatrix} \sin(2\omega t) \\ -\cos(2\omega t) \end{bmatrix} \tag{44}$$

The negative and positive sequences are represented using the equations (44) and (43). The instantaneous PQ theory equations attained from park's transformation by substitution of decoupled current and voltage values is given as,

$$P_1 = \frac{3}{2}[V_{d1} \quad -V_{q1} \quad V_{d2} \quad V_{q2}] \begin{bmatrix} i_{q2} \\ i_{d2} \\ i_{q1} \\ i_{d1} \end{bmatrix} \tag{45}$$

$$Q_1 = P_2 = \frac{3}{2}[V_{d1} \quad V_{q1} \quad V_{d2} \quad V_{q2}] \begin{bmatrix} i_{d2} \\ i_{q2} \\ i_{d1} \\ i_{q1} \end{bmatrix} \tag{46}$$

$$Q_2 = \frac{3}{2}[V_{d1} \quad -V_{q1} \quad V_{q2} \quad -V_{d2}] \begin{bmatrix} i_{q2} \\ i_{d2} \\ i_{d1} \\ i_{q1} \end{bmatrix} \tag{47}$$

On the basis of decoupled current and voltage, the reference signal produced is given as,

$$P_0 = \frac{3}{2}[V_{d1} \quad -V_{q1} \quad -V_{d2} \quad V_{q2}] \begin{bmatrix} i_{q2} \\ i_{d2} \\ i_{q1} \\ i_{d1} \end{bmatrix} \tag{48}$$

$$Q_0 = P_2 = \frac{3}{2}[V_{d1} \quad V_{q1} \quad V_{d2} \quad V_{q2}] \begin{bmatrix} i_{d2} \\ i_{q2} \\ i_{d1} \\ i_{q1} \end{bmatrix} \tag{49}$$
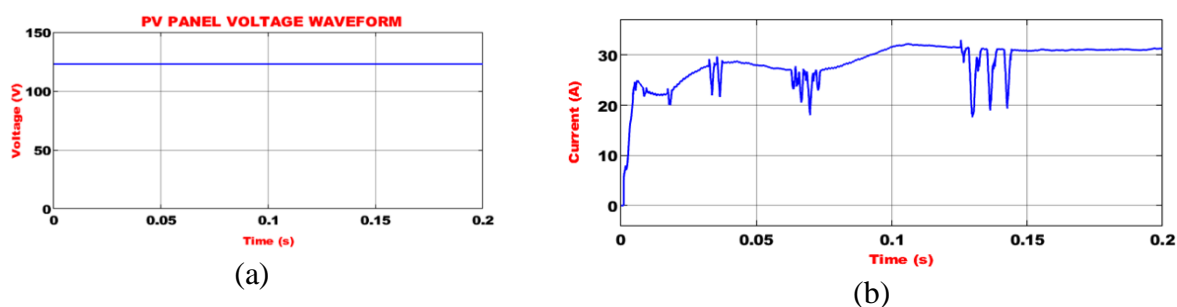
Thus the reference voltage and reference current for compensating the source voltage fluctuations and load current harmonics is attained by using DDSRF theory.

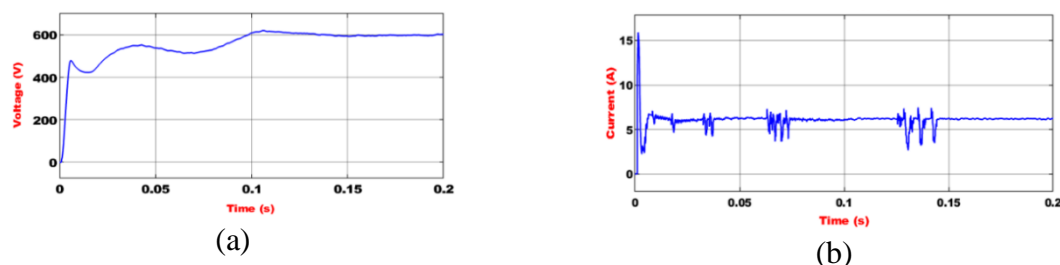## IV   RESULTS AND DISCUSSIONS

Due to the increased incidence of sensitive loads in the distributed power system, the need for enhanced PQ is drawing significant amount of attention recently. As a result, this work presents the implementation of a PV-UPQC with appropriate control measures for improving the PQ. An adaptive PI controller is used for stabilizing the enhanced voltage output derived from the Re-lift Luo converter, which interfaces the PV with the UPQC. Additionally, the CT2FLC in addition to DDSRF theory used for the control of UPQC.

1918

Eur. Chem. Bull. 2023,12(5), 1906-1924

Table 1: Parameter Specifications

Parameters	Specifications
PV panel	
Power	$10\,kW$
No. of PV panels	$500\,W, 20\,panels$
V_{SC}	12 V
V_{OC}, I_{SC}	$22.6\,V, 41.6\,A$
Re-lift Luo converter	
Inductors L_a, L_b, L_c	$3\,mH$
Capacitors C_a, C_b, C_c	$22\,\mu F$
Capacitors C_o	$2200\,\mu F$
Power switch	IGBT
Switching frequency	$10\,kHz$

(a)

(b)

Figure 10: Waveforms of (a) PV panel voltage (b) PV panel current

In order to obtain a higher DC output voltage, the re-lift Luo converter is supplied with an input of 125 V from the PV panel, as shown in Figure 10(a). The Figure 10(b) shows that the PV panel output current experiences abrupt changes as a result of the various operating conditions before reaching a stable output current of about 32 A.

(a)

(b)

Figure 11: Waveforms of (a) Converter output voltage and (b) Converter output current

The re-lift Luo converter gives out a stable output voltage and output current of 600 V and 7 A, respectively, with the aid of an adaptive PI controller as illustrated in Figure 11.
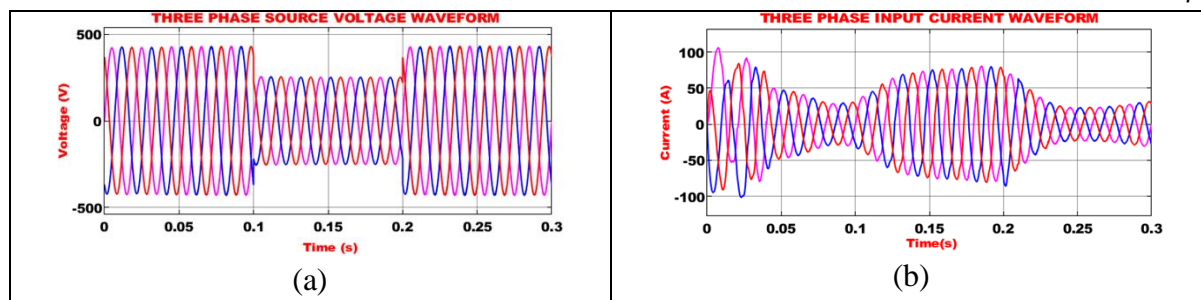
1919

Figure 12: Waveforms of (a) Three phase source voltage and (b) Three phase source current

From Figure 12 (a), it is clear that about 400 V AC voltage is constantly maintained up to 0.1 s and due to the influence of PQ issues, the voltage drops to 250 V after 0.1s. As illustrated in Figure 12 (b), the three phase source current exhibits distortion and is highly unstable due to the presence of PQ issues.
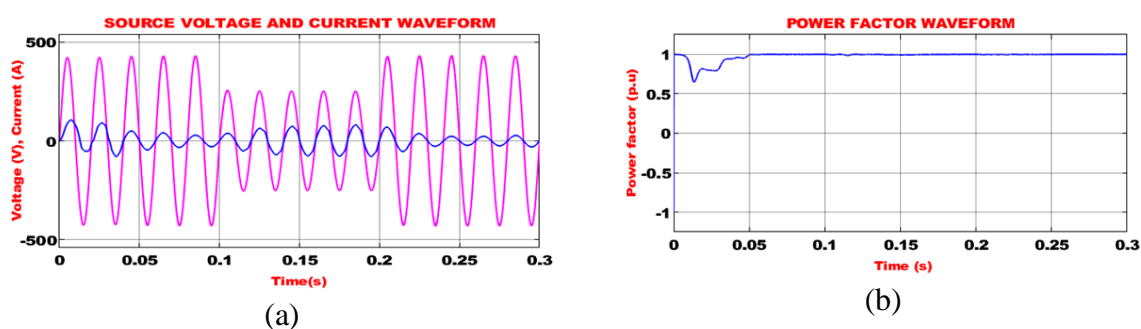

Figure 13: Waveforms of (a) Source voltage and current (b) Power factor

It is clear from Figure 13 (b) that CT2FLC-based UPQC effectively improves power quality and aids for the achievement of unity power factor. The waveforms of source voltage and current are illustrated in Figure 13 (a).
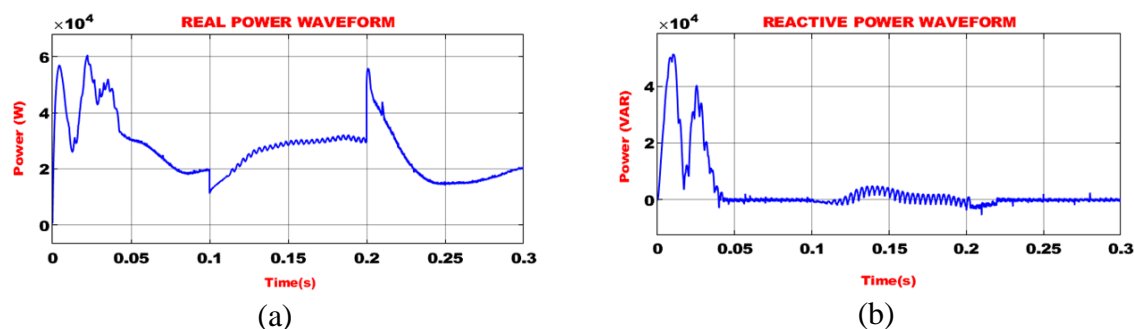

Figure 14: Waveforms showing (a) real power and (b) reactive power

Real power and reactive power are depicted in Figures 14 (a) and 14 (b), respectively. Power fluctuations are visible in the waveform at first, but after applying the proposed control technique, the real and reactive power are distortion-free.
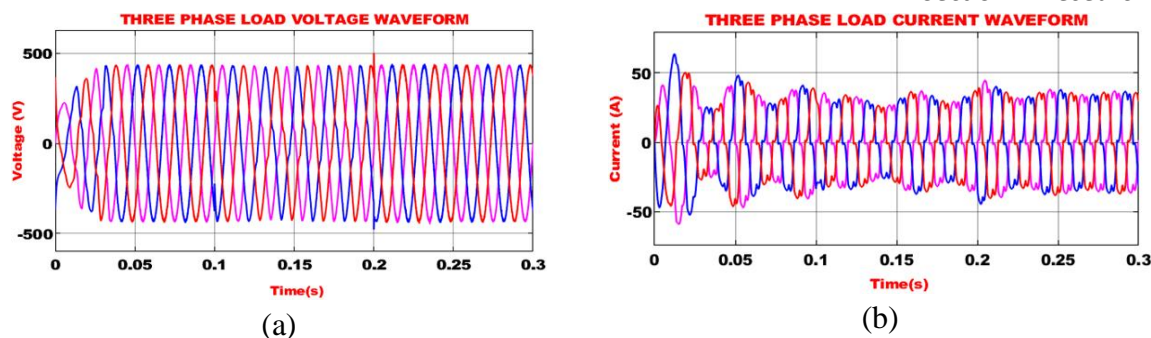
1920

(a)

(b)

Figure 15: Waveforms showing (a) load voltage and (b) load current

With the proposed PQ enhancement technique, a stable load voltage of 400 V and a load current of about 35 A are constantly maintained with no distortions. Hence, the proposed PV-UPQC with CT2FLC configuration effectively and successfully improves the PQ on the load side as shown in Figure 15.
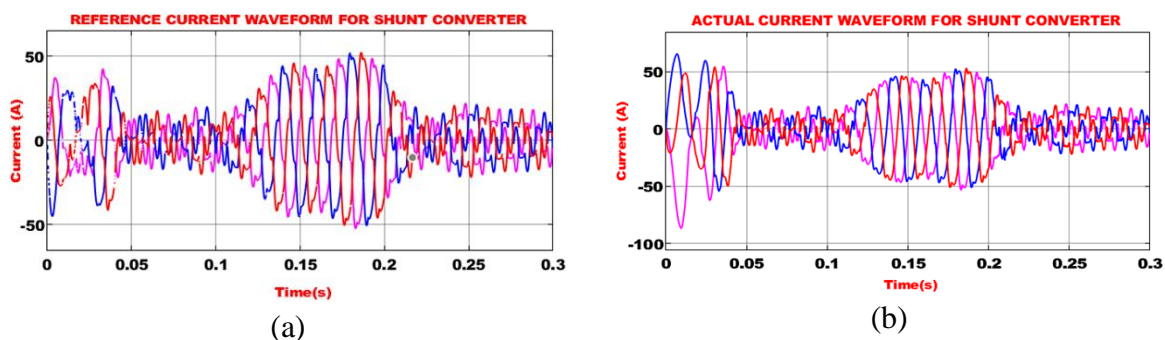

(a)

(b)

Figure 16: Waveforms of (a) Reference current and (b) actual current for shunt converter

With the injection of desired magnitude of reactive current in to the line, effective load current harmonics compensation is achieved using a shunt converter, which functions as a controllable current source. A reference current of 45 A is generated between 0.15s and 0.2s in order to reduce the current harmonics that are present on the load side as shown in Figure 16 (a).
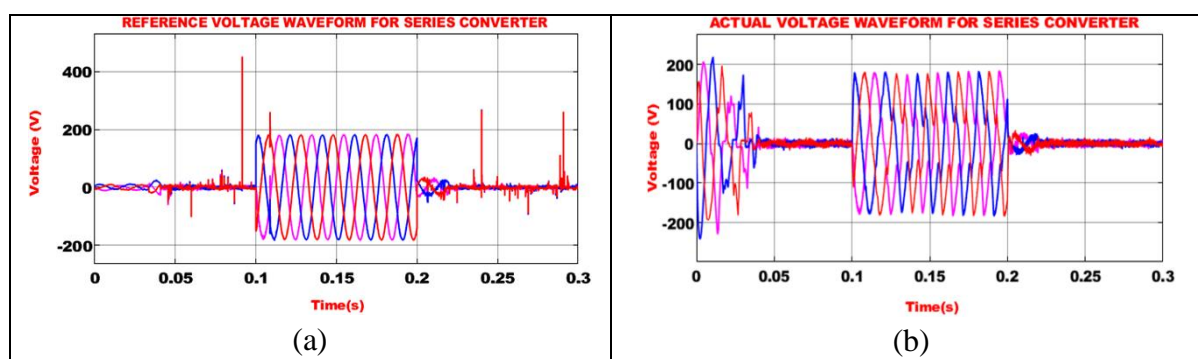

(a)

(b)

Figure 17: Waveforms of (a) Reference voltage and (b) actual voltage for series converter

With the injection of desired magnitude of voltage in to the line, effective voltage sag compensation is achieved using a series converter. As shown in the Figure 17 (b), a constant voltage of 180 V is obtained without any distortions from 0.1s to 0.2s. A THD of 3.25% is estimated as seen in Figure 18.
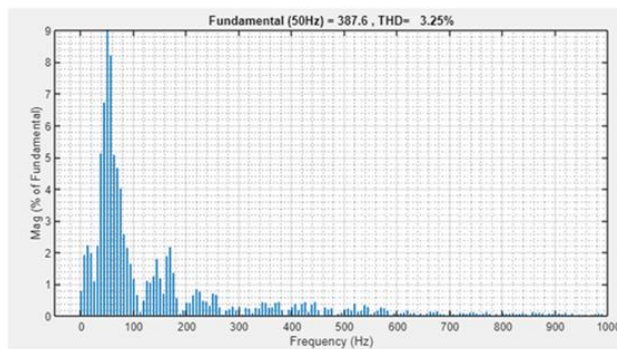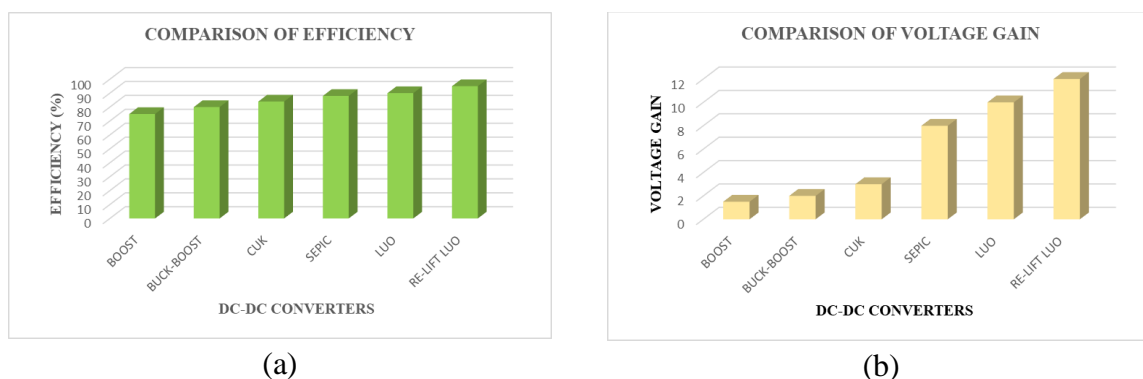
Figure 18: THD waveform

| (a) | (b) |

Figure 19: Comparison of: (a) Efficiency and (b) Voltage gain

As shown in Figure 19, the operational performance of the Re-lift Luo converter is compared to a number of other existing converters on the basis of voltage gain and efficiency. The Re-lift Luo converter performs exceptionally well with an excellent voltage gain ratio of 1:12 and efficiency of 95%.

V   CONCLUSION

Due to the increasing application of sensitive power electronic devices, various PQ issues have arisen in power systems. These problems could eventually result in significant economic loss due to entire system failure if they are not effectively resolved. A PV based power generation combined with UPQC provide a clean energy with improved PQ. The PV system, as an intermittent low power source, causes voltage instability. The re-lift Luo converter along with the adaptive PI controller improves and stabilizes the voltage generated from the PV. Moreover, the control of the UPQC is ensured using CT2FLC and DDSRF theory. The designed UPQC configuration is effective in enhancing both the load side and source side PQ issues on the basis of the output obtained from MATLAB simulations. The Re-lift Luo converter possesses a high voltage gain of ratio 1:12 and impressive efficiency of 95%.

REFERENCES

1. Montoya, Francisco G., Raul Baños, Alfredo Alcayde, Maria G. Montoya, and Francisco Manzano-Agugliaro. "Power quality: Scientific collaboration networks and research trends." *Energies* 11, no. 8: 2067, 2018.

1922

Eur. Chem. Bull. 2023,12(5), 1906-1924

2. Xi, Yanhui, Zewen Li, Xiangjun Zeng, Xin Tang, Qiao Liu, and Hui Xiao. "Detection of power quality disturbances using an adaptive process noise covariance Kalman filter." *Digital Signal Processing* 76: 34-49, 2018.

3. S. Devassy and B. Singh, "Design and Performance Analysis of Three-Phase Solar PV Integrated UPQC," in *IEEE Transactions on Industry Applications*, vol. 54, no. 1, pp. 73-81, Jan.-Feb. 2018.

4. Bollen, Math HJ, and Irene YH Gu. *Signal processing of power quality disturbances*. John Wiley & Sons, 2006.

5. Singh, Bhim, Ambrish Chandra, and Kamal Al-Haddad. *Power quality: problems and mitigation techniques*. John Wiley & Sons, 2014.

6. Kumar Agarwal, Rahul, Ikhlaq Hussain, and Bhim Singh. "Three- phase single- stage grid tied solar PV ECS using PLL- less fast CTF control technique." *IET Power Electronics* 10, no. 2: 178-188, 2017.

7. N. Beniwal, I. Hussain and B. Singh, "Second-Order Volterra-Filter-Based Control of a Solar PV-DSTATCOM System to Achieve Lyapunov's Stability," in *IEEE Transactions on Industry Applications*, vol. 55, no. 1, pp. 670-679, Jan.-Feb. 2019.

8. G. Modi, S. Kumar and B. Singh, "Improved Widrow–Hoff Based Adaptive Control of Multiobjective PV-DSTATCOM System," in *IEEE Transactions on Industry Applications*, vol. 56, no. 2, pp. 1930-1939, March-April 2020.

9. J. Ye and H. B. Gooi, "Phase Angle Control Based Three-phase DVR with Power Factor Correction at Point of Common Coupling," in *Journal of Modern Power Systems and Clean Energy*, vol. 8, no. 1, pp. 179-186, January 2020.

10. A. Moghassemi, S. Padmanaban, V. K. Ramachandaramurthy, M. Mitolo and M. Benbouzid, "A Novel Solar Photovoltaic Fed TransZSI-DVR for Power Quality Improvement of Grid-Connected PV Systems," in *IEEE Access*, vol. 9, pp. 7263-7279, 2021.

11. E. M. Molla and C. -C. Kuo, "Voltage Sag Enhancement of Grid Connected Hybrid PV-Wind Power System Using Battery and SMES Based Dynamic Voltage Restorer," in *IEEE Access*, vol. 8, pp. 130003-130013, 2020.

12. P. Ray, P. K. Ray and S. K. Dash, "Power Quality Enhancement and Power Flow Analysis of a PV Integrated UPQC System in a Distribution Network," in *IEEE Transactions on Industry Applications*, vol. 58, no. 1, pp. 201-211, Jan.-Feb. 2022.

13. J. Yu, Y. Xu, Y. Li and Q. Liu, "An Inductive Hybrid UPQC for Power Quality Management in Premium-Power-Supply-Required Applications," in *IEEE Access*, vol. 8, pp. 113342-113354, 2020.

14. Sefa, I., N. E. C. M. İ. Altin, S. Ozdemir, and O. R. H. A. N. Kaplan. "Fuzzy PI controlled inverter for grid interactive renewable energy systems." *IET Renewable Power Generation* 9, no. 7: 729-738, 2015.

15. Juang, C-F., and C-F. Lu. "Load-frequency control by hybrid evolutionary fuzzy PI controller." *IEE Proceedings-generation, transmission and distribution* 153, no. 2: 196-204, 2006.

16. Bayhan, Sertac, Sevki Demirbas, and Haitham Abu- Rub. "Fuzzy- PI- based sensorless frequency and voltage controller for doubly fed induction generator connected to a DC microgrid." *IET Renewable Power Generation* 10, no. 8: 1069-1077, 2016.

1923

17. Kaya, Ibrahim. "Improving performance using cascade control and a Smith predictor." *ISA transactions* 40, no. 3: 223-234, 2001.

1924

Eur. Chem. Bull. 2023,12(5), 1906-1924